Biochimica et Biophysica Acta 812 (1985) 9–20
Elsevier

BBA 72409

A kinetic model for *N*-ethylmaleimide inhibition of the $(Na^+ + K^+)$-ATPase from rectal glands of *Squalus acanthias*

Mikael Esmann and Jens G. Nørby

Institute of Biophysics, University of Aarhus, DK-8000 Aarhus C (Denmark)

(Received July 13th, 1984)

Key words: $(Na^+ + K^+)$-ATPase; *N*-Ethylmaleimide; (*S. acanthias*)

(1) The time-course of inhibition by *N*-ethylmaleimide (NEM) of $(Na^+ + K^+)$-ATPase and K^+-*p*-nitrophenylphosphatase activity of $(Na^+ + K^+)$-ATPase from *Squalus acanthias* has been followed over a 4000-fold inhibitor concentration range. The $(Na^+ + K^+)$-ATPase and the K^+-*p*-nitrophenylphosphatase were inhibited in parallel at all inhibitor concentrations. (2) The data obtained have led to a model with the following features. (a) The enzyme is inactivated via two routes in which the reactivities towards NEM are different. This can explain that about 80% of the activity disappears 40–1000-times faster than the remaining 20%. (b) A primary reaction of SH groups with NEM without inhibition which is required before (c) a subsequent rection with NEM and inhibition can take place (i.e., a lag period). (d) A complicated concentration dependence of the rates of inactivation in the rapid phase which is interpreted in terms of an additional equilibrium between two different enzyme conformations. (3) The results are compatible with our previous finding (Esmann, M. (1982) Biochim. Biophys. Acta 688, 260–270) that more than one SH group per enzyme molecule are modified when the enzyme is inactivated.

Introduction

The role of the sulphydryl groups for the catalytic activity of the $(Na^+ + K^+)$-ATPase (EC 3.6.3.1) has been studied using a number of probes such as *N*-ethylmaleimide (NEM), dithionitrobenzoic acid, nucleotide analogs and mercuro compounds as well as fluorescent derivatives of these (see Refs. 1–10 and references therein). The modes of inactivation of the enzyme by these probes have given information on different ligand-induced conformational states of the enzyme. A detailed kinetic analysis of the interaction between the inhibitors and the enzyme has not, however, been performed previously.

We have recently used NEM as a reagent for modification of the SH groups of the $(Na^+ + K^+)$-ATPase, and the biphasic inactivation of the enzyme led us to classify the SH groups in terms of their importance for the catalytic activity [8–10]. According to this classification, class I contains two SH groups per α-chain (M_r 104000) and these groups can be modified with NEM without loss of enzymatic activity. Class II consists of four SH groups per α-chain, and the modification of these groups with NEM leads to an enzyme preparation with about 20% activity. Class III contains SH groups which react slowly with NEM (compared to class II), and the modification of the class III groups finally leads to complete inactivation of the enzyme preparation.

In the present paper we propose a minimal model for the inactivation of the $(Na^+ + K^+)$-ATPase and K^+-*p*-nitrophenylphosphatase activ-

Abbreviations: NEM, *N*-ethylmaleimide; DTNB, 5,5′-dithiobisnitrobenzoic acid; α-subunit, the 104 kDa peptide; CDTA, *trans*-1,2-cyclohexylenedinitrilotetraacetic acid.

ity of $(Na^+ + K^+)$-ATPase from *Squalus acanthias* by NEM. The model is based on an extensive kinetic study and it is compatible with the above-mentioned incorporation studies and the resulting classification of the sulphydryl groups involved.

Materials and Methods

$(Na^+ + K^+)$-ATPase is prepared from rectal glands of *S. acanthias* as previously described [11] and the membrane-bound enzyme used in these experiments has a specific $(Na^+ + K^+)$-ATPase activity of 1370 μmol/mg protein per h and a specific K^+-activated *p*-nitrophenylphosphatase activity of 205 μmol/mg per h. These activities correspond to 100% in the figures.

Incubation of enzyme with NEM is carried out at 37°C in the presence of 150 mM KCl, 5 mM CDTA and 30 mM Tris-HCl buffer (pH 7.0 at 37°C). The protein concentration in the incubation medium is between 0.02 and 0.1 mg/ml, equal to an enzyme concentration of 0.05–0.25 μM [11]. The lower protein concentrations are used at the lower NEM concentrations (2.5–10 μM) to ensure a large molar excess of NEM over enzyme. The incubation is initiated by the addition of 1 vol. NEM in water to 1 vol. of a vigorously stirred enzyme suspension, giving the above-mentioned final concentrations. The reaction mixture is stirred throughout the incubation period. An aliquot is taken at the desired time points and transferred to an ice-cold solution of 10 mM mercaptoethanol/25% glycerol/20 mM histidine (pH 7.0). Control experiments show that the reaction of enzyme with NEM is completely and immediately quenched by mercaptoethanol. The $(Na^+ + K^+)$-ATPase and the K^+-*p*-nitrophenylphosphatase activities are then measured as previously described [9]. All activities are given as percentage of the activity before the addition of NEM. Control experiments showed that there is no appreciable hydrolysis of NEM during the incubation (see Ref. 9) and that the spontaneous inactivation of the enzyme at 37°C is negligible under the conditions used here (not shown).

Results

The aim of the present paper is to characterize qualitatively and quantitatively the kinetics of the inactivation by NEM of the $(Na^+ + K^+)$-ATPase activity and the K^+-*p*-nitrophenylphosphatase activity of $(Na^+ + K^+)$-ATPase from the rectal gland of *S. acanthias*.

To this purpose the time-course of inactivation was followed for up to 1 h at 37°C in the presence of 150 mM KCl and with NEM concentrations from 2.5 μM to 10 mM (10000 μM). The results are given in Figs. 1, 2 and 3, and they show the following characteristic qualitative features. (a) As observed earlier (e.g., Fig. 4 in Ref. 9), the rate of inactivation is dependent on NEM concentration; and (b) the semilogarithmic plots reveal that the inactivation is biphasic, with about 80% of the

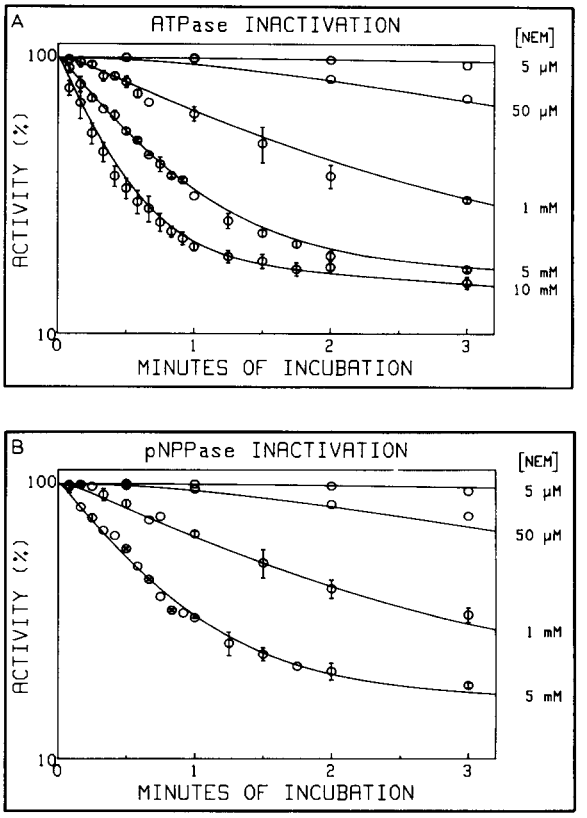

Fig. 1. Time-course of NEM inhibition of the $(Na^+ + K^+)$-ATPase and the K^+-*p*-nitrophenylphosphatase activities. Enzyme was incubated with the indicated concentrations of NEM and the enzymatic activity was measured at the time points indicated as described in Materials and Methods. The error bars give the S.D. of 3–5 independent experiments. The curves are drawn according to the mathematical expression given in Fig. 7 with the rate constants shown in Fig. 6. The ordinate is logarithmic.

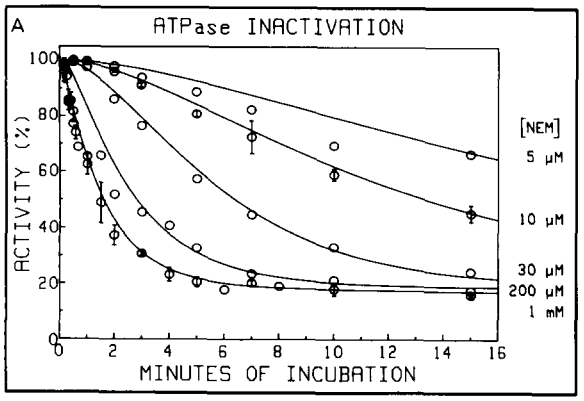

Fig. 2. Time-course of NEM inhibition of the $(Na^+ + K^+)$-ATPase and the K^+-*p*-nitrophenylphosphatase activity. These curves illustrate the lag period. Experimental details as given in the legend to Fig. 1.

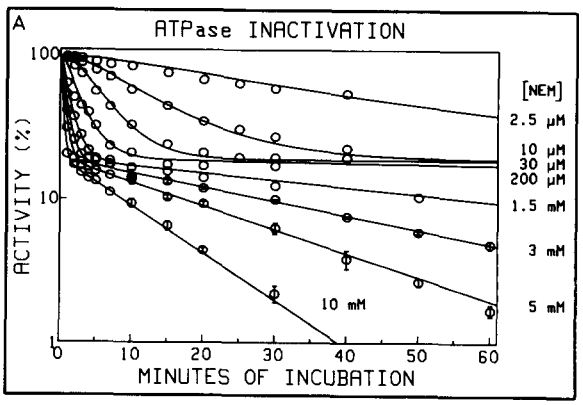

Fig. 3. Complete time-course of NEM inhibition of the $(Na^+ + K^+)$-ATPase and the K^+-*p*-nitrophenylphosphatase activity. Experimental details as given in the legend to Fig. 1.

activity being lost relatively quickly (Fig. 3), this proportion being independent of the concentration of NEM, at least over a range of 3 orders of magnitude (10 μM to 10 mM). Furthermore (c), there is an observable lag period (e.g., Fig. 2), at least with the low concentrations of NEM.

It is obvious from Fig. 3, that the slow inactivation of about 20% of the activity can be described as a monoexponential decay, and a preliminary analysis showed that the pseudo-first-order rate constant for the slow phase was proportional to [NEM] (see Fig. 5A). The rapid inactivation phase, isolated by subtraction of the slow phase (see below), also appeared to be monoexponential (at least for [NEM] > 10 μM, see Fig. 4). However, a complex dependence of the rate constant on [NEM] was observed for the rapid phase (Fig. 5B). Fig. 5 clearly illustrates the justification for the distinction between 'slow' and 'rapid' phases of inactivation. The ratio of the observed rate constant for the rapid phase to that for the slow is about 40 at high [NEM], and up to about 10^3 at low [NEM]. Note that this preliminary analysis neglects the presence of the lag period in the inactivation, that is apparent at low NEM concentrations, e.g., Figs. 2 and 3.

A kinetic model for the inactivation of $(Na^+ + K^+)$-ATPase by NEM

In evaluating the model that will explain the time-course (lag period, biphasic inactivation) as well as the NEM concentration dependence of the inactivation, we have proceeded in two steps.

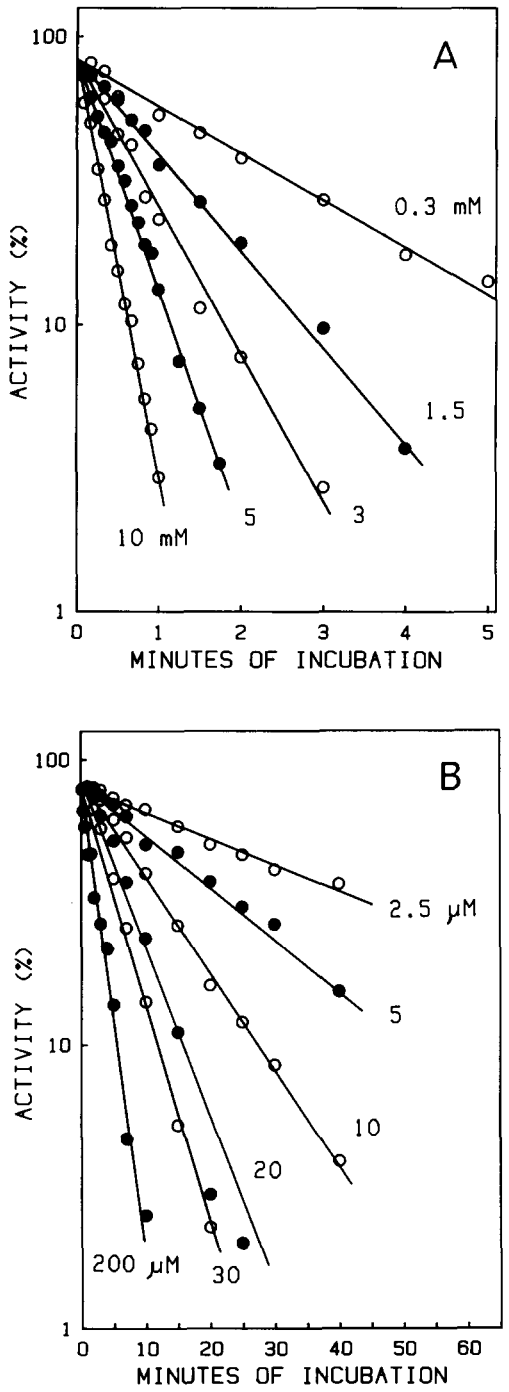

Fig. 4. Time-course of NEM inhibition of the $(Na^+ + K^+)$-ATPase activity illustrating the rapid phase of inactivation. The data from Figs. 1–3 are replotted after subtraction of the slow phase (see text for further details). The straight lines intersecting the ordinate at 81% are drawn by eye. The NEM concentrations are given in the figure (mM in panel A; μM in panel B).

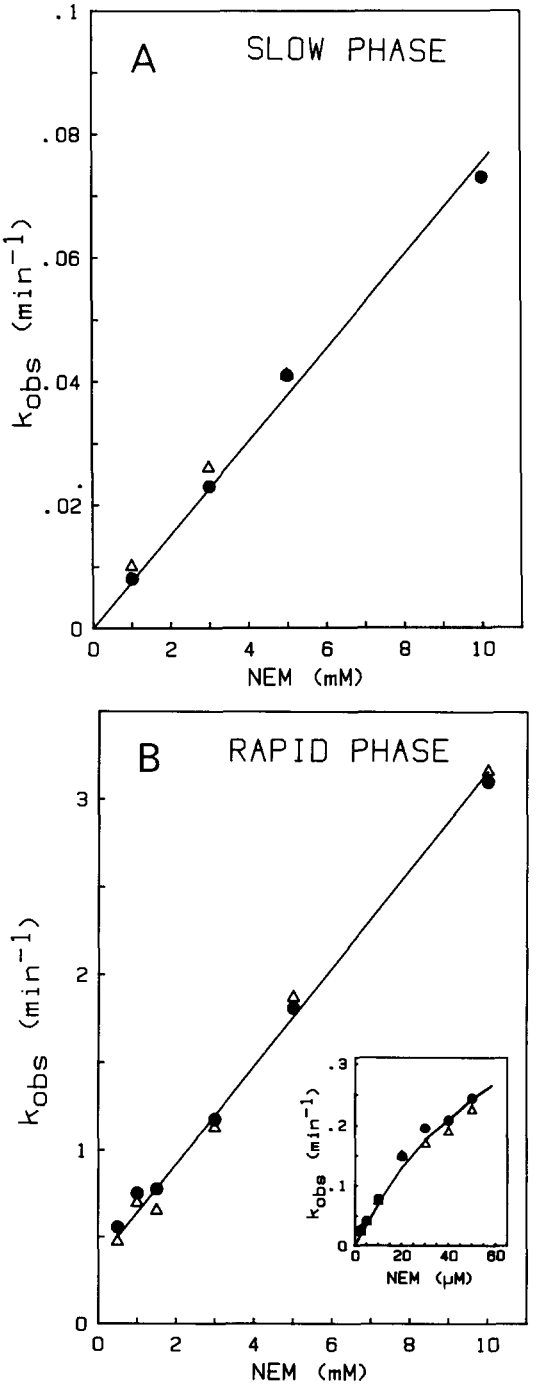

Fig. 5. Concentration dependence of the observed first-order rate constants for NEM inhibition of $(Na^+ + K^+)$-ATPase (●) and K^+-*p*-nitrophenylphosphatase (△) for the slow phase of inactivation (panel A), and for the rapid phase of inactivation (panel B). The rate constant, k_{obs}, is obtained from Fig. 4 for the rapid phase and the inset shows k_{obs} at the lowest NEM concentrations. k_{obs} for the slow phase of inactivation is obtained from Fig. 3. Note the 35-fold difference between ordinates of the panel A and B.

(1) An explanation of the biphasic inactivation

In the first step we consider various models that can explain the fact that, irrespective of [NEM], about 80% of the activity disappears much more quickly than the remaining 20%. The simplest explanation is of course, that the enzyme preparation is heterogeneous, consisting of 80% of one and 20% of another ($Na^+ + K^+$)-ATPase, i.e., 80% E_A and 20% E_B (with very little variation from preparation to preparation). Although we cannot at present exclude entirely this possibility, we judge it unlikely for these reasons. There are several similarities between control enzyme and enzyme modified with NEM in the presence of 150 mM K^+, 150 mM Na^+ or 150 Na^+ + 3 mM ATP to about 80% inactivation. The partially NEM-inhibited enzyme has the same molar activity (activity per phosphorylation site, Table I, Ref. 8) and the same cation activation characteristics (see Fig. 9 in Ref. 1) as the control. Furthermore, the K^+- and ADP-sensitivity of the mixture of phosphorylated enzyme intermediates, EP, is the same for the control and the partially inhibited preparations (Fig. 1, Ref. 8). We therefore feel compelled to construct a model that can accommodate the biphasic inactivation of a homogeneous enzyme preparation.

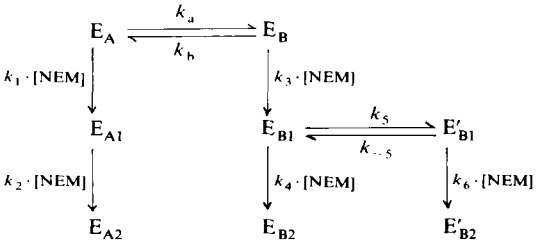

$k'_1 = 1.99$ $mM^{-1} \cdot min^{-1}$
$k_2 = 0.0076$ $mM^{-1} \cdot min^{-1}$
$k'_3 = 8.5$ $mM^{-1} \cdot min^{-1}$
$k_4 = 0.269$ $mM^{-1} \cdot min^{-1}$
$k_5 = 0.42$ min^{-1}
$k_{-5} = 7.6$ min^{-1}
$k_6 = 2000$ $mM^{-1} \cdot min^{-1}$

Fig. 6. A model for the reactions with NEM leading to inhibition of the ($Na^+ + K^+$)-ATPase and K^+-*p*-nitrophenylphosphatase. The native enzyme is supposed to be in a rapid equilibrium between E_A and E_B. Reaction of E_A with NEM leads to inactivation along the slow route, whereas reaction with E_B leads to inactivation along the rapid route (see text). The rate constants k_a, k_b, k_5 and k_{-5} (in min^{-1}) are independent of [NEM]; all others have the dimension $mM^{-1} \cdot min^{-1}$ and the values used in the curve fittings in Figs. 1–3 are given below. The rate constants k_a and k_b are assumed to be always much larger than $k_1 \cdot [NEM]$ and $k_3 \cdot [NEM]$, and k'_1 and k'_3 are defined as $k_1 k_b/(k_a + k_b)$ and $k_3 k_a/(k_a + k_b)$ respectively, see Appendix. Enzyme species E_{A2}, E_{B2} and E'_{B2} are inactive (and possibly identical) and all other have full enzymatic activity.

For the reasons just mentioned, we also exclude a sequential model for the inactivation: $E \rightarrow E(NEM) \rightarrow E(NEM)_2 \rightarrow E(NEM)_3$ where E and E(NEM) are fully active, whereas $E(NEM)_2$ has a molar activity which is 20% of control and $E(NEM)_3$ is inactive.

In the Appendix we consider three simple models that may explain the biphasic inactivation pattern. The first model represents inhomogeneity of the preparation and, as discussed above, we consider that unlikely. Of the other two models, which are mathematically identical (see Appendix), we have chosen No. 2, since it has the least internal constraints. This model, with an extra branch (E'_{B1}, E'_{B2}) added, is shown in Fig. 6. The extra branch is the result of the second step in the evaluation of the data.

(2) Interpretation of the relation between the NEM concentration and the observed rate constants

As outlined in the Appendix for model 2 (which is equivalent to Fig. 6 without the E'_{B1}, E'_{B2} branch) the enzyme activity is proportional to:

$$[E_A] + [E_B] + [E_{A1}] + [E_{B1}] = [E] + [E_{A1}] + [E_{B1}];$$

$$[E] = [E_A] + [E_B]$$

In this model, $k_2 \ll k'_1 + k'_3$ (see Appendix and Fig. 6) and the time functions for the different active enzyme species are given by:

$$[E] = e^{-(k'_1 + k'_3)[NEM]t} \quad (1)$$

$$[E_{A1}] = \frac{k'_1}{k'_1 + k'_3} \cdot e^{-k_2[NEM]t} - \frac{k'_1}{k'_1 + k'_3} \cdot e^{-(k'_1 + k'_3)[NEM]t} \quad (2)$$

$$[E_{B1}] = \frac{k'_3}{k'_1 + k'_3 - k_4} \cdot (e^{-k_4[NEM]t} - e^{-(k'_1 + k'_3)[NEM]t}) \quad (3)$$

Since k_2 is much smaller than $k'_1 + k'_3$ the function characterizing the monoexponential part of

the slow inactivation (Figs. 3 and 5A) via route A must be:

$$[E_{A1}] = \frac{k'_1}{k'_1 + k'_3} \cdot e^{-k_2[NEM]t} \quad (4)$$

As the intercept of this function with the y-axis is $k'_1/(k'_1 + k'_3)$ we have from Fig. 3 that $k'_1/(k'_1 + k'_3) = 0.19$ or $k'_3/k'_1 = 4.3$. The second-order rate constant, k_2, is determined from Fig. 5A to be 0.0076 $mM^{-1} \cdot min^{-1}$.

In an attempt to characterize separately the rapid phase, we have subtracted the activity corresponding to Eqn. 4 from the total activity ($E + E_{A1} + E_{B1}$) whereby we get what we here call 'the corrected activity'. The mathematical expression for this is:

$$\text{Act.(corr)} = \frac{k'_3}{k'_1 + k'_3 - k_4} \cdot e^{-k_4[NEM]t} - \left(\frac{k'_3}{k'_1 + k'_3 - k_4} - \frac{k'_3}{k'_1 + k'_3} \right) \cdot e^{-(k'_1 + k'_3)[NEM]t} \quad (5)$$

In Fig. 4 'the corrected activity' is plotted versus time for [NEM] equal to 2.5 μM–10 mM. As a first (and obviously quite good) approximation, these curves may be considered as monoexponential with an ordinate intercept equal to 0.81. In Fig. 5B the apparent rate constant (k_{obs}, min^{-1}) obtained from Fig. 4 is plotted versus [NEM] (mM), and it appears that k_{obs} is a linear function of [NEM] for [NEM] $\geq$ 0.5 mM:

$$k_{obs} = 0.4 + 0.27[NEM] \ (min^{-1}) \quad (6)$$

whereas at very low [NEM] (under 0.02 mM), k_{obs} approaches the relation (see inset in Fig. 5B):

$$k_{obs} = 10[NEM] \ (min^{-1}) \quad (7)$$

However, the theoretical expression (Eqn. 5) corresponding to model 2 (Appendix) is neither monoexponential, nor can it satisfy Eqns. 6 and 7. In two obvious cases will Act(corr) be a monoexponential function (after a short time), namely if k_4 is much larger than $k'_1 + k'_3$:

$$\text{Act(corr)} \approx \frac{k'_3}{k'_1 + k'_3} \cdot e^{-(k'_1 + k'_3)[NEM]t} \quad (5a)$$

or if $k_4 \ll k'_1 + k'_3$:

$$\text{Act(corr)} \approx \frac{k'_3}{k'_1 + k'_3} \cdot e^{-k_4[NEM]t} \quad (5b)$$

where, in both cases, $k'_3/(k'_1 + k'_3) = 0.81$. Under both these conditions, however, k_{obs} should be proportional to [NEM] and that is in contrast to the observations – see Eqn. 6 which is derived from Fig. 5B.

We therefore propose the modification of model 2 shown in Fig. 6 with the corresponding equations in Fig. 7. Route A still represents the slow phase and E_A, E_{A1}, E_B, E_{B1} and E'_{B1} are all active.

The E_{B1}-E'_{B1}-E'_{B2} branch provides the means by which the observed relation in Eqn. 6 can be satisfied, since it contains an NEM-independent isomerization: Namely if $k_6 \gg k_4$, then at high [NEM], where we can make $k_6 \cdot [NEM] \gg k_5$, the observed rate constant for inhibition will be:

$$k_{obs} = k_5 + k_4 \cdot [NEM] \ (\text{high } [NEM]) \quad (6a)$$

When we compare this with the observed relation (Eqn. 6) we obtain the values $k_5 = 0.4$ min^{-1} and $k_4 = 0.27$ $mM^{-1} \cdot min^{-1}$.

Note that the requirement for an NEM-independent step in route B automatically excludes the possibility that $k_4 \gg k'_1 + k'_3$ (see above, Eqn. 5a) and a natural second assumption is therefore $k_4 \ll k'_1 + k'_3$.

Computer simulation of the inactivation

Following the reasoning above, the mathematical expressions (Fig. 7) corresponding to the model in Fig. 6 were now used to determine the rate constants by trial and error. By means of a numerical integration procedure analogous to the one described by Nørby et al. [12] the equations in Fig. 7 lead to the curves given in Figs. 1–3. As mentioned, obvious starting values for the simulation are: $k_2 = 0.0076$ $mM^{-1} \cdot min^{-1}$, $k_4 = 0.27$ $mM^{-1} \cdot min^{-1}$, $k_5 = 0.4$ min^{-1}. Furthermore, $k'_3/k'_1 = 4.3$. With regard to the relationship of k_{obs} at very low [NEM] (see inset Fig. 5B and Eqn. 7) to the constants in the model, there are as a first approximation two possibilities: either k'_3 or k_6 must be about 10 $mM^{-1} \cdot min^{-1}$. Both situations were simulated. By far the best fit, especially to the experiments with the intermediate NEM con-

$$[E]_{t+dt} = [E]_t - (k_1' + k_3') \cdot [NEM] \cdot [E]_t \cdot dt; \quad ([E] = [E_A] + [E_B])$$

$$[E_{A1}]_{t+dt} = [E_{A1}]_t + (k_1' \cdot [NEM] \cdot [E]_t - k_2 \cdot [NEM] \cdot [E_{A1}]_t) \cdot dt$$

$$[E_{B1}]_{t+dt} = [E_{B1}]_t + (k_3' \cdot [NEM] \cdot [E]_t + k_{-5} \cdot [E'_{B1}]_t - (k_5 + k_4 \cdot [NEM]) \cdot [E_{B1}]_t) \cdot dt$$

$$[E'_{B1}]_{t+dt} = [E'_{B1}]_t + (k_5 \cdot [E_{B1}]_t - (k_{-5} + k_6 \cdot [NEM]) \cdot [E'_{B1}]_t) \cdot dt$$

$$k_1' = k_1 \cdot k_b / (k_a + k_b) \text{ and } k_3' = k_3 \cdot k_a / (k_a + k_b)$$

$$\text{Enzyme activity} = [E] + [E_{A1}] + [E_{B1}] + [E'_{B1}]$$

Fig. 7. Equations describing the time dependence of the catalytically active enzyme species shown in Fig. 6.

centrations (50–1000 μM), was obtained with k_3' = 8.5 $mM^{-1} \cdot min^{-1}$ and $k_6 \gg k_3'$. The conversion of E_{B1} to E'_{B1} was initially assumed to be irreversible (and NEM-independent), i.e., $k_{-5} = 0$, but although this allowed satisfactory simulation of the data, an experiment described below suggests that k_{-5} is much greater than k_5. In the simulation of the different possibilities, k_5 was held constant at 0.4 min^{-1} (see above) and only the values of k_{-5} and k_6 were varied.

An experiment suggesting an E_{B1}-E'_{B1} equilibrium

Having determined the rate constants except k_{-5} and k_5 for the model in Fig. 6 we designed an experiment to determine the approximate value of k_{-5}, especially to see whether $k_{-5} = 0$ or $k_{-5} \gg k_5$.

The enzyme was incubated with 200 μM NEM for 2 min and the reaction was then immediately quenched with mercaptoethanol, see Methods. The enzyme was then washed three times by centrifugation to remove mercaptoethanol. Under these incubation conditions $k_3' \cdot [NEM] = 2\ min^{-1}$, $k_4 \cdot [NEM] = 0.05\ min^{-1}$ and $k_5 = 0.4\ min^{-1}$, i.e., E_{B1} should be produced and no appreciable loss of activity should occur, even if E_{B1} were subsequently converted to E'_{B1}, since E'_{B1} is still active (Fig. 6). Accordingly the activity of the prelabelled enzyme was 90–95% of the control. When this preincubated enzyme was subsequently incubated with 20 μM NEM, a time-course of inhibition (not shown) qualitatively similar to that expected from the results in Fig. 1–3 was obtained, but without the lag period. The rate constant corresponding to the rapid phase was about 0.45 min^{-1} and thus very close to k_5 (Fig. 6).

These results exclude the possibility of an irreversible, NEM-independent step from E_{B1} to E'_{B1} (Fig. 6). In that case, the preincubated enzyme, which after preincubation was without NEM for a period sufficient to allow complete conversion (k_5 = 0.4 min^{-1}, i.e., $t_{1/2} < 2$ min) of E_{B1} to E'_{B1}, would denature with the rate constant $k_6 \cdot [NEM]$. The minimum value for k_6 (corresponding to $k_{-5} = 0$) was found to be about 135 $mM^{-1} \cdot min^{-1}$. If the preincubated enzyme had converted to E'_{B1} the enzyme should denature with a rate constant of at least 7 min^{-1} at 20 μM NEM, and not 0.45 min^{-1} as observed. In fact, the conclusion must be that there is an equilibrium between E_{B1} and E'_{B1}, with very little E'_{B1} in the preparation after prelabelling with NEM and standing and that, therefore, $k_{-5} \gg k_5$.

In summary, this experiment, besides elucidating the problem of reversibility between E_{B1} and E'_{B1}, directly supports the model in Fig. 6. The lag period, originating in the proposed step from E_B to the still active E_{B1} was eliminated by preincubation and the resulting preparation had a rate constant for the rapid inactivation phase close to that predicted by the model.

Discussion

The present paper provides a detailed, quantitative study of the inhibitory effect of NEM on ($Na^+ + K^+$)-ATPase, with the purpose of modelling the involvement of SH groups in both the ($Na^+ + K^+$)-ATPase and the K^+-*p*-nitrophenylphosphatase activity.

The first qualitatively striking feature of the inactivation time-course is that it is biphasic in a

semilog plot, showing initially a rapid phase followed by a slower one. It is well known that detailed and extensive inactivation curves (Figs. 1–3) are a prerequisite for a differential modelling of enzyme inactivation (see, for example, Refs. 13–15). Furthermore, it is of importance for our interpretation that we have measured the detailed inactivation time-course using a 4000-fold concentration range of NEM – from 2.5 to 10000 μM. This has enabled us to assure quantitatively that the intercept with the ordinate (log scale) of the slow monoexponential inactivation phase is completely independent of [NEM] (see Fig. 3). This result places decisive constraints with regard to the models that may simulate the data. A third, qualitative characteristic is the occurrence of a lag period, as shown especially in Figs. 2 and 3.

As discussed in the Results section, the simplest models that may explain the above-mentioned independence of the ordinate intercept on NEM are models 2 and 3 in the Appendix. With the expansion (the E_{B1}-E'_{B1} branch) the final scheme shown in Fig. 6 becomes the minimal model that can simulate all our data.

The part of the model that is decisive for the NEM-independent proportion of the the two routes of denaturation is the rapid equilibrium between the unmodified species E_A and E_B, including the special relation between k_1, k_3 and k_a and k_b (see Fig. 6 and Appendix). Model 3 (Appendix) has no isomerization step, but the unreacted enzyme possesses two SH groups with different reactivity in the first steps. The ratio of the rate constants k_1, and k_3, $k_3/k_1 = 4.3$ will here determine the 'pool sizes'. It must be pointed out that the forms E_A and E_B in our model are distinguished only by their SH group reactivity, and bear no relation to the isomers usually denoted E_1 and E_2.

The proportion of enzyme denatured along the two routes is not only independent of NEM, but also of the specific ligands (Na^+, K^+ and ATP) present during incubation with NEM. This means, that although these ligands affect the rate of denaturation, e.g., the magnitude of k_2 and k_6, they do not change k'_1/k'_3 (see Ref. 10).

Although the model shown is a sequential reaction scheme we cannot exclude that E_A and E_B are denatured directly by the same processes and the same rate constants as E_{A1} and E_{B1} ($k_2 \cdot$ [NEM] and $k_4 \cdot$ [NEM]). Inclusion of this possibility would not influence the computation of denaturation curves, since k'_1 and k'_3 are much larger than k_2 and k_4. It is, in fact, an attractive assumption that the properties of the catalytically important SH groups are not changed by the reactions from E_A to E_{A1} and E_B to E_{B1}. The enzymatic properties of the dominant species after 80% inactivation, E_{A1}, seems to be exactly the same as those of the native enzyme [8], and E_{B1} also resembles native enzyme at least with regard to the turnover numbers for ($Na^+ + K^+$)-ATPase and K^+-*p*-nitrophenylphosphatase activity, see Results.

The kinetic model and the SH groups of Classes I, II and III

The model in Fig. 6 shows that each enzyme molecule in the course of inactivation reacts with at least two NEM molecules. In this connection we note that the blocking by NEM of the two SH groups of class I (see Ref. 9) is not included in the scheme, since these groups are without importance both for activity and for the subsequent pattern of NEM incorporation [9] and inactivation (data not shown). Reaction of NEM with the approximately four SH groups previously designated to class II leads to a preparation with about 20% of the original activity [9], the apparent rate constant of the inactivation and the NEM incorporation being the same [10]. In the model in Fig. 6, the steps involved must be all those leading from E_A and E_B to E_{A1}, E_{B2} and E'_{B2}. The fact that these steps taken together only involve about two reactions with NEM per molecule in our model, whereas four SH-groups * were found in the incorporation study [10] does not make the two studies incompatible. The following two reasons can be given for the two studies being compatible.

Firstly, with K^+ alone, as in the present study, reaction of the four SH groups in class II with NEM leads to a rapid loss of activity and also of the enzyme's ability to be phosphorylated, form

* Due to the uncertainty of the actual NEM concentration in radiolabelling experiments (see Ref. 5) we have also titrated the SH groups in the native enzyme with DTNB and correlated the labelling of the enzyme and the loss of activity. We find – in agreement with our NEM-labelling measurements [10] – that three or four SH groups are labelled with DTNB at the same rate as the activity is lost (data not shown).

EP, from Na^+, Mg^{2+} and ATP. If ATP is present together with K^+ during the incubation with NEM, only about three SH groups are found in class II, but activity is lost in parallel with their blockage [10]. The inactive enzyme can, however, be phosphorylated with Na^+, Mg^{2+} and ATP [8]. To describe this, we resolve the reaction $E_{B1} \rightarrow E_{B2}$ in our model (Fig. 6) into two steps: $E_{B1} \rightarrow E_{B12} \rightarrow E_{B2}$ and likewise for $E_{A1} \rightarrow E_{A2}$ and $E'_{B1} \rightarrow E'_{B2}$. The intermediaries E_{B12}, E'_{B12} and E_{A12} (not shown in Fig. 6) then represent inactive enzyme still capable of being phosphorylated, whereas all catalytic properties and partial reactions have disappeared when E_{B1}, E_{B2} and E_{A2} (Fig. 6) are reached. Thus expanded, our scheme would show a minimum of three reactions with NEM per molecule.

Secondly, one must bear in mind that it is impossible to ascertain that each of the reactions in Fig. 6 involve only one SH group: There might very well be two or more identical groups that react in, for example, the step from E_{B1} to E_{B2}.

Our interpretation is further substantiated when we compare our model with the studies with spin labelled NEM [9,10]. These reveal the presence of two types of SH group in class II. There seems to be one mobile SH group and one or more SH groups that are restricted in their movements. One might speculate that the mobile SH group is the one reacting with a high rate constant (k'_1 or k'_3) in the steps $E_A \rightarrow E_{A1}$ and $E_B \rightarrow E_{B1}$, whereas the restricted groups, one of which is protected by ATP (see Ref. 10 and above), are the less reactive ones, involved in the subsequent reactions leading to inactive enzyme and loss of ability to phosphorylate.

The class III groups will be those blocked by NEM concomitant with the slow inactivation step $E_{A1} \rightarrow E_{A2}$.

The reaction scheme proposed in Fig. 6 is clearly complex, and ligand-induced changes in denaturation rates are not easily related to specific steps in the model. Therefore, extensive studies over large concentration and time ranges will be required to obtain a quantitative description of the SH groups related to conformational changes and catalytic activity. For example, the rate of denaturation is lower in NaCl than in KCl [1,5,10,18], but only an extensive study could tell whether it is k_4, k_5, k_{-5} or k_6 that is changed by replacing K^+ with Na^+.

Comparison with other studies

The characteristic biphasic pattern of inactivation reported here for shark ($Na^+ + K^+$)-ATPase has also been observed when enzyme prepared from brain was incubated with NEM at 37°C [1,2,16]. Here about 60% of the activity disappeared rapidly and 40% slowly. In contrast, there are several studies reporting a monoexponential time-course for the inactivation of kidney ($Na^+ + K^+$)-ATPase [5,18,19]. None of these studies included a variation in the concentration of NEM, and kinetic schemes for the inactivation were therefore not reported. Interpreted from our scheme in Fig. 6, the variation in inactivation pattern might be due to a species or tissue dependent position of the $E_A \rightleftharpoons E_B$ equilibrium as well as different relative values for k_1 and k_3. In this connection it is important to note that the inactivation has not been followed to less than 10–20% residual activity in previous studies. If $k_1 k_b/(k_a + k_b) \ll k_3 k_a/(k_a + k_b)$, then such studies might show monoexponential time-courses and yet be compatible with our model. In a recent study (unpublished data) we have observed a 'slow' component, comprising only 3–4% of the total ($Na^+ + K^+$)-ATPase (or K^+-*p*-nitrophenylphosphatase) activity when kidney enzyme is incubated with 5–20 mM NEM. The small magnitude could explain why this has not been reported before.

In the present study we observe a parallel decrease in the ($Na^+ + K^+$)-ATPase and K^+-*p*-nitrophenylphosphatase activities. However, partial activities such as phosphorylation, ATP and ouabain binding as well as ATP/ADP exchange do not necessarily decrease in parallel with the ($Na^+ + K^+$)-ATPase activity. The denaturation pattern is dependent not only on the ligands present [9,18,19] but also on the type of SH reagent; see, for example, Refs. 17, 20, 21.

In a study of the NEM inactivation of the ($Na^+ + K^+$)-ATPase from kidney, Winslow [5] has correlated loss of activity with incorporation of NEM into the α-chain. An incorporation of NEM into three or four SH groups per α-chain was observed, with two or three of these reacting more

rapidly than the remainder. This is compatible with both the model (Fig. 6) presented here and with our previous measurement [10] of incorporation of NEM into the α-chain.

Conclusion

Based on our results and the discussion above we shall propose that the reaction scheme detailed in Fig. 6 is a valid minimal model for the involvement of SH groups in catalysis by the ($Na^+ + K^+$)-ATPase: Two SH groups react rapidly with NEM, leading to an enzyme (E_{A1}, E_{B1}, E'_{B1}) whose catalytic properties are unchanged even though its reactivity towards NEM may have changed. In subsequent reactions with NEM, involving two or three groups, the enzyme first loses its ($Na^+ + K^+$)-ATPase activity (E_{A12}, E_{B12}, E'_{B12}, not shown in Fig. 6, but see Discussion above) and then all its catalytic properties. Probably only the last reaction involves an SH group on the ATP-binding site.

Appendix

Three simple models that explain the biphasic inactivation pattern

We shall briefly discuss three models that may explain that about 80% of the activity disappears much more quickly than the remaining 20%, irrespective of the NEM concentration and irrespective of the nature of the ligands present during inactivation (150 mM $K^+ \pm 3$ mM ATP or 150 mM $Na^+ \pm 3$ mM ATP; this paper and Ref. 9).

These models illustrate either an inhomogeneity in the preparation (model 1) or a branched mechanism allowing the enzyme to be denatured along two routes (models 2 and 3). The left branch, A, is defined at the slowest route. All active species are assumed to have the same turnover number, the total activity thus being proportional to the sum of their concentrations. In all these preliminary, simple models the right branch, B, must subsequently be modified (see text) to include the special dependence of the fast phase on [NEM] (see, for example, Fig. 5B).

In model 1, E_A is 18–20% of $E_A + E_B$, and both E_{A1} and E_{B1} are inactive. k_3 is much larger than k_1. It is evident that the time-course of denaturation of such a heterogeneous enzyme mixture as

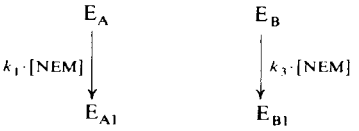

Model 1.

described by model 1 will be a sum of two exponentials:

$$[E_A]+[E_B] = [E_A]_0 \cdot e^{-k_1[NEM]t} + [E_B]_0 \cdot e^{-k_3[NEM]t}$$

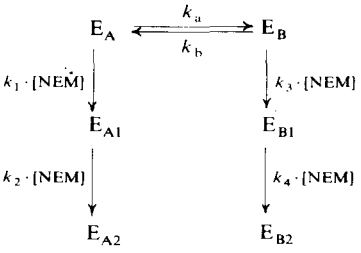

Model 2.

In model 2, E_A, E_B, E_{A1} and E_{B1} all have full activity, whereas E_{A2} and E_{B2} are inactive. 18–20% of the activity disappears via route A.

The conditions under which model 2 can simulate the quantitative distribution ($R = 0.19/0.81 = 0.23$) between slowly inactivated (route A) and rapidly inactivated enzyme (route B) can be determined using the general analytical expression for a two compartment model (see, for example, Klodos et al., Ref. 22). It can be shown that:

$$R = \frac{[E_{A2}]_\infty}{[E_{B2}]_\infty} = \frac{k_1 k_b \cdot (k_a + k_b + k_3 \cdot [NEM])}{k_3 k_a \cdot (k_a + k_b + k_1 \cdot [NEM])}$$

R will show the required independence of [NEM] under three conditions:

(1) if $k_3 \cdot [NEM]$ and $k_1 \cdot [NEM]$ are always much larger than k_a and k_b then R will be k_b/k_a. If this is to be valid also at the lowest NEM concentrations, model 2 becomes virtually identical to the 'heterogeneity' model 1.

(2) if $k_3 = k_1$ then R is likewise k_b/k_a.

(3) if k_a and/or k_b are always much larger than $k_1 \cdot [NEM]$ and $k_3 \cdot [NEM]$, then R is $k_1 k_b / k_3 k_a$.

Since this is the model evaluated in the main text, we shall consider it in some detail here. Following the analysis of Klodos et al. [22], case 2

and 3 leads to a condition where $[E_A]/[E_B]$ is independent of time. Using assumption 3 above in the further analysis and defining:

$$k_1' = k_1 \cdot \frac{k_b}{k_a + k_b};$$

$$k_3' = k_3 \frac{k_a}{k_a + k_b}$$

and

$$[E] = [E_A] + [E_B];$$

$$[E] + [E_{A1}] + [E_{B1}] + [E_{B2}] = 1$$

we have

$$[E] = e^{-(k_1 + k_3') \cdot [NEM] \cdot t} \tag{2.1}$$

$$[E_{A1}] = \frac{k_1'}{k_1' + k_3' - k_2} \cdot (e^{-k_2 \cdot [NEM] \cdot t} - e^{-(k_1' + k_3') \cdot [NEM] \cdot t}) \tag{2.2}$$

$$[E_{B1}] = \frac{k_3'}{k_1' + k_3' - k_4} \cdot (e^{-k_4 \cdot [NEM] \cdot t} - e^{-(k_1' + k_3') \cdot [NEM] \cdot t}) \tag{2.3}$$

These expressions are used in the primary kinetic evaluation in the text. Note that the maximal rate constant for inactivation via either branch is $(k_1' + k_3')[NEM]$. This means that the rate constant for the inactivation in the slow phase (route A, mono-exponential) must be $k_2[NEM] \ll (k_1' + k_3')[NEM]$, and therefore E_{A1} can be written:

$$[E_{A1}] = \frac{k_1'}{k_1' + k_3'} (e^{-k_2 [NEM] t} - e^{-(k_1' + k_3')[NEM] t}) \tag{2.4}$$

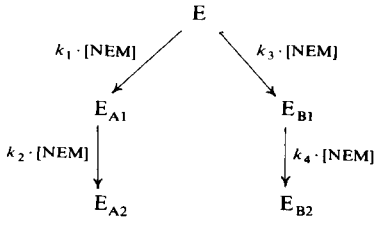

Model 3.

In model 3, E, E_{A1} and E_{B1} all have full and unmodified activity, whereas E_{A2} and E_{B2} are inactive. k_3 is about $4.3 \cdot k_1$ (see text).

In model 3 it is assumed that E has two types of SH group with different 'reactivity' as $k_3 = 4.3 \cdot k_1$ and thus about 20% of the enzyme will be inactivated through route A. The equations corresponding to model 3 are as 2.1, 2.3 and 2.4 except that k_1' and k_3' are substituted with k_1 and k_3.

In both of the models 2 and 3, which are mathematically indistinguishable, the relative rates of inactivation are determined by k_4/k_2, which will be larger than 30 (see Results). The expanded mechanism that will explain the detailed inactivation pattern is discussed under Results using model 2 as a basic model (see Fig. 6, main text).

Acknowledgements

This work has been supported financially by P. Carl Petersens Foundation, The Danish Medical Research Council and 'Ingeborg and Leo Dannin's Foundation for Medical Research'. Ms. Angielina Tepper is thanked for excellent technical assistance.

References

1 Skou, J.C. (1974) Biochim. Biophys. Acta 339, 234–245
2 Hara, S., Hara, Y., Nakao, T. and Nakao, M. (1981) Biochim. Biophys. Acta 644, 53–61
3 Patzelt-Wenczler, R. and Schoner, W. (1981) Eur. J. Biochem. 114, 79–87
4 Patzelt-Wenczler, R. and Mertens, W. (1981) Eur. J. Biochem. 121, 197–202
5 Winslow, J.W. (1981) J. Biol. Chem. 256, 9522–9531
6 Taniguchi, K., Suzuki, K. and Iida, S. (1982) J. Biol. Chem. 257, 10659–10667
7 Koepsell, H., Hulla, F.W. and Fritsch, G. (1982) J. Biol. Chem. 257, 10733–10741
8 Esmann, M. and Klodos, I. (1983) Curr. Topics Membranes Transp. 19, 349–352
9 Esmann, M. (1982) Biochim. Biophys. Acta 688, 251–259
10 Esmann, M. (1982) Biochim. Biophys. Acta 688, 260–270
11 Skou, J.C. and Esmann, M. (1979) Biochim. Biophys. Acta 567, 436–444
12 Nørby, J.G., Klodos, I. and Christiansen, N.O. (1983) J. Gen. Physiol. 82, 725–759
13 Ray, J.R., Jr. and Koshland, D.E., Jr. (1961) J. Biol. Chem. 236, 1973–1979
14 Kenney, W.C. (1975) J. Biol. Chem. 250, 3089–3094
15 Le-Quoc, K., Le-Quoc, D. and Gaudemer, Y. (1981) Biochemistry 20, 1705–1710

16 Patzelt-Wenczler, R., Pauls, H., Erdmann, E. and Schoner, W. (1975) Eur. J. Biochem. 53, 301–311
17 Takeguchi, C., Honegger, K.E., Holland, W.W. and Titus, E.O. (1976) Life Sci. 19, 797–806
18 Schoot, B.M., Schoots, A.I.M., De Pont, J.J.H.H.M., Schuurmans Stekhoven, F.M.A.H. and Bonting, S.L. (1977) Biochim. Biophys. Acta 483, 181–192
19 Wallick, E.T., Anner, B.M., Ray, M.V. and Schwartz, A. (1978) J. Biol. Chem. 253, 8778–8786
20 Askari, A., Huang, W. and Henderson, G.R. (1979) in Na,K-ATPase: Structure and Kinetics (Skou, J.C. and Nørby, J.G., eds.), pp. 205–215, Academic Press, New York
21 Hansen, O., Jensen, J. and Ottolenghi, P. (1979) in Na,K-ATPase: Structure and Kinetics (Skou, J.C. and Nørby, J.G., eds.), pp. 217–226, Academic Press, New York
22 Klodos, I., Nørby, J.G. and Plesner, I.W. (1981) Biochim. Biophys. Acta 643, 463–482